

A simulation study of some observable parameters of Cherenkov photons in EASs of different primaries incident at various angles

G. S. Das*, P. Hazarika† and U. D. Goswami‡

Department of Physics, Dibrugarh University, Dibrugarh 786 004, Assam, India

We have studied the lateral density, arrival time and angular distributions of Cherenkov photons in Extensive Air Showers (EASs) initiated by γ -ray, proton and iron primaries incident with different energies and at different zenith angles. This study is the extension of our earlier work [1] to cover almost the whole energy range of ground based γ -ray astronomy and to cover a wide range of zenith angles ($\leq 40^\circ$), as well as the extension to study the angular distribution patterns of Cherenkov photons in EASs. This type of study is important for distinguishing the γ -ray initiated showers from the hadronic showers in the ground based γ -ray astronomy, where Atmospheric Cherenkov Technique (ACT) is used. Importantly, such study gives an insight on the nature of γ -ray and hadronic showers in general. In this work, we used the CORSIKA 6.990 simulation package for the generation of EASs. Similar to the case of Ref.[1], this study also revealed that, the density and arrival time distribution profiles of Cherenkov photons follow the almost exponentially decreasing and increasing functions respectively with different values of the functions' parameters according to the type, energy and angle of incidence. The angular distribution shows a linear decrease in density with respect to the angle of incidence. Most of the photons are scattered within 1° to 2° from the shower axis. There is no significant difference in the results obtained by using the QGSTJETII and EPOS high energy hadronic interaction models.

PACS numbers: 95.55.Ka, 98.70.Rz, 41.60.Bq, 91.10.Vr

I. INTRODUCTION

In the ground based γ -ray astronomy, the Atmospheric Cherenkov Technique (ACT) is most extensively used to detect γ -rays from celestial sources in the energy range of few hundred GeV to few TeV. The ACT is based on detection of Cherenkov photons emitted in the Extensive Air Showers (EASs) created during the process of interaction between the primary γ -rays and earth's atmosphere [2]. It is important to note that, the sources which emit γ -rays also emit Cosmic Rays (CRs). As the CRs are charged particles, they got deflected by the intergalactic magnetic fields and hence they lose their directional property, whereas γ -rays being neutral, retain their direction of origin. So the detection of γ -rays can lead to the estimation of the locations of such astrophysical objects.

ACT, being an indirect process of γ -ray detection and due to the presence of huge CR background, a detailed Monte Carlo simulation studies of atmospheric Cherenkov photons have to be carried out for detection and proper estimation of their energy from the observational data of experiments based on ACT. Although both γ -ray and CR can generate EAS, the nature of two are different as the former is purely electromagnetic in nature, whereas the later is an admixture of electromagnetic and hadronic cascades. Many studies have already been carried out, specially on the lateral density and arrival time distributions of Cherenkov photons in EASs using available detailed simulation techniques [3–7]. However, not many studies have been done on angular distributions as well as on lateral density and arrival time distributions of Cherenkov photons, initiated by γ -ray and hadronic particles, incident at various zenith angles with a wide range of energy, particularly at high altitude observation levels. This is the extension of our earlier work [1] to cover almost the whole energy range of ground based γ -ray astronomy and to cover a wide range of zenith angles ($\leq 40^\circ$), as well as the extension to study the angular distribution patterns of Cherenkov photons in EASs. So, in this work we have studied the lateral density, arrival time and angular distributions of Cherenkov photons at different energies and zenith angles over a high altitude observation level, using two different high energy hadronic interaction models, viz., QGSTJETII and EPOS with FLUKA low energy hadronic interaction model available in the CORSIKA simulation package [8].

CORSIKA is a four dimensional detailed Monte Carlo simulation package developed to study the evolution and properties of extensive air showers in the atmosphere. It allows to simulate interactions and decays of nuclei, hadrons, muons, electrons and photons in the atmosphere upto energies of some 10^{20} eV. Presently, CORSIKA has the option of seven high energy hadronic interaction models and three low energy hadronic interaction models for the simulation of hadronic interactions [8]. However, for the simulation of electromagnetic component of the air shower, it uses the EGS4 code [9].

The rest of the paper is organized as follows. In the Section II, we discuss about the simulation process. The Section III contains the analysis and results of the work. Finally, the work is summarized in the Section IV.

* gsdas@dibru.ac.in

† poppyhazarika1@gmail.com

‡ umananda2@gmail.com

II. SIMULATION OF EXTENSIVE AIR SHOWERS

The simulation of Cherenkov photons in EAS is carried out by using the CORSIKA 6.990 simulation package. As mentioned earlier, we have used two high energy hadronic interaction models, viz., QGSJETII.3 and EPOS 1.99 with the low energy hadronic interaction model FLUKA to generate EASs for the monoenergetic γ -ray, proton and iron primaries incident vertically as well as inclined at zenith angles 10° , 20° , 30° and 40° . We use two high energy hadronic interaction models to have greater acceptability of our work and this will also provide an opportunity to compare the performance of the models concerned. The reason of selection of QGSJETII and EPOS high energy hadronic interaction models is that, QGSJETII is the improved version of the model QGSJET 01, and EPOS is based on quantum mechanical multiple scattering approach based on partons and strings, which performed better in comparison to RHIC data [10]. In our earlier work [1], we have studied extensively the QGSJET01C, VENUS 4.12 and QGSJETII.3 along with all low energy hadronic interaction models presently available in CORSIKA. By using QGSJETII-FLUKA and EPOS-FLUKA model combinations, the following numbers of showers were generated at different energies and zenith angles for the γ -ray, proton and iron primaries as given in the Table I.

TABLE I: Number of showers generated at different energies for the γ -ray, proton and iron primaries incident at 0° , 10° , 20° , 30° and 40° zenith angles.

Primary particle	Energy	Number of Showers
γ -ray	100 GeV	10000
	250 GeV	7000
	500 GeV	5000
	1 TeV	2000
	2 TeV	1000
Proton	250 GeV	10000
	500 GeV	8000
	1 TeV	5000
	2 TeV	2000
	5 TeV	800
Iron	5 TeV	4000
	10 TeV	2000
	50 TeV	1000
	100 TeV	600

The range of energies of the primaries selected for this work are the typical ACT energy range of respective primaries in terms of the equivalent number of Cherenkov photons yield. The altitude of HAGAR experiment at Hanle (longitude: $78^\circ 57' 51''$ E, latitude: $32^\circ 46' 46''$ N, altitude: 4270 m) is used as the observational level in the generation of these showers. The core of the EASs is considered to be at the centre of the detector array. The detector geometry is set as a horizontal flat detector array, where there are 25 telescopes in the E–W direction with a separation of 25 m and 25 telescopes in the N–S direction with a separation of 20 m. The mirror area of each telescope is taken as 9 m^2 . For the longitudinal distribution of Cherenkov photons, photons are counted only in the step where they are emitted and the Cherenkov light emission angle is chosen as wavelength independent. The wavelength window for the Cherenkov radiation produced is selected as 200 – 650 nm and only those charged particles generated by photons within the specified range propagates to the ground before absorption. The position and time (with respect to the first interaction) of each photon hitting the detector on the observation level are recorded. The variable bunch size option of Cherenkov photon is set to "5", to reduce the data size. Multiple scattering length for e^- and e^+ is decided by the parameter STEPFC in EGS code [9], which has been set to 0.1. The low energy cutoff's for the particle kinetic energy is chosen for hadrons, muons, electrons and photons as 3.0, 3.0, 0.003 and 0.003 GeV respectively. The US standard atmosphere parametrized by Linsley has been used [11].

III. ANALYSIS AND RESULTS

The lateral density of the Cherenkov photon is obtained by counting the numbers of photons generated per shower and incident on each detector. The arrival time of the Cherenkov photon is the time taken by the photon to reach a detector with respect to the first photon of the shower hitting the array. After which the average of these arrival times is taken, as there are several photons hitting each detector per shower. Since there are shower to shower fluctuations in Cherenkov photon density and arrival time at each detector, the variation of Cherenkov photon density and arrival time with core distance is obtained by calculating average values over the specified number of showers. The fluctuations of photon density and arrival time as a function of core distance (or for each detector) is shown by calculating the ratio of their r.m.s to mean values. The angular distribution of Cherenkov photons is obtained by counting the number of photons produced per angular bin with respect to the shower axis and then averaged over the azimuth. Also, to investigate the model dependent variations of these parameters, as in the case of our earlier work [1], the percentage relative deviations between the two models with respect to the corresponding parameters is calculated by using the

following formula:

$$\Delta_{\xi} = \frac{\xi_{mp} - \xi_{rp}}{\xi_{rp}} \times 100\%, \quad (1)$$

where Δ_{ξ} is the percentage relative deviation of the parameter, and ξ_{rp} and ξ_{mp} are the reference model parameter and the given model parameter respectively.

The analysis has been done by using C++ programs on the ROOT software [12] platform. The various aspects of lateral density, arrival time and angular distributions of Cherenkov photons and their model dependent behaviours are discussed in the following subsections:

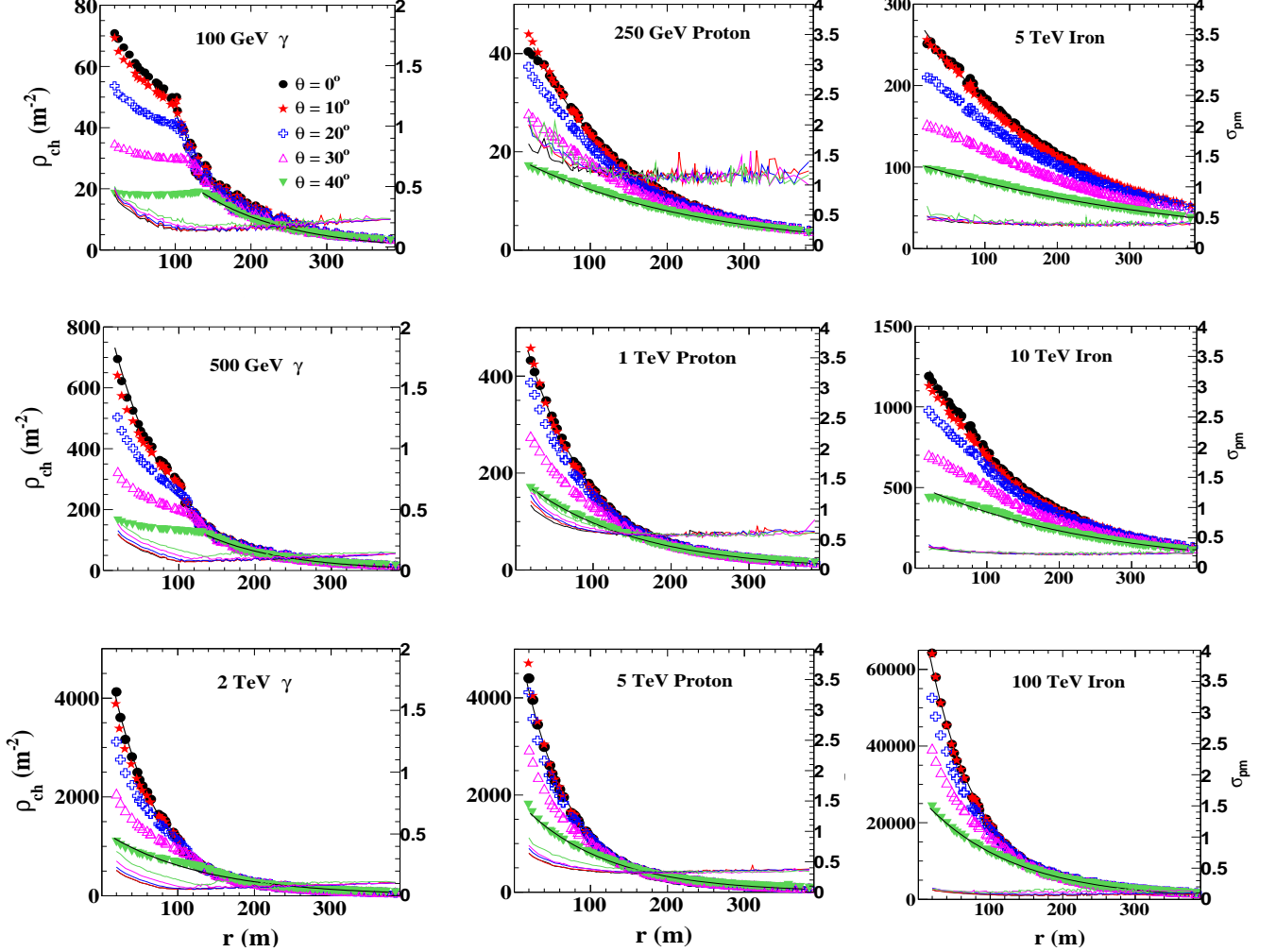


FIG. 1: Average Cherenkov photon densities (ρ_{chs}) and their r.m.s. values per mean (σ_{pms}) with respect to distance from the shower core of γ -ray, proton and iron primaries for different energies and angle of incidences. The solid lines in respective plots indicate the results of the best fit function (2).

A. Lateral density of Cherenkov photon

1. General characteristics

The variations of average Cherenkov photon densities (ρ_{chs}) and their r.m.s. values per mean (σ_{pms}) as a function of core distance for the EPOS-FLUKA model combination is shown in the Fig.1. To save the space, in this figure, we have shown the plots only at three different energies for all three primaries, viz. for γ , proton and iron primaries incident vertically as well as inclined at zenith angles 10° , 20° , 30° and 40° respectively. It is observed that, the distribution of ρ_{chs} falls off exponentially with core distance, for all primary particles and their energies with gradual reduction in the slope with increase in the angle of incidence. The variation may be effectively represented by the equation [1]

$$\rho_{ch}(r) = \rho_0 e^{-\beta r}, \quad (2)$$

where $\rho_{ch}(r)$ is the position dependent density function of Cherenkov photons, r is the distance from the shower core, ρ_0 is the coefficient and β is the slope of the function. Different primaries will have different values of ρ_0 and β depending upon their energy and the angle of incidence. As an example, the best fit negative exponential functions, represented by the equation (2), for the vertically incident and for the most inclined (i. e. incident at 40°) showers are shown by the solid lines in the plots of the Fig.1. Fittings are done by using the χ^2 -minimization method in the ROOT software [12] platform. However, due to the presence of the significant characteristic hump for 100 GeV γ -ray primary, the fit is not proper. For the vertically incident primary, this hump is observed at a core distance of around 100 m. With increasing zenith angle (θ), the distance of the hump from the core increases with increasing prominence, even the hump is seen upto the energy of 1 TeV for the $\theta = 40^\circ$. Although, the distributions follow the same mathematical function almost for all the cases with different coefficients and slopes, the geometry of the distributions is different for different primaries at a particular energy and at a particular θ . It is seen that at a given energy and θ , the distribution shows a larger curvature for the γ -ray primary (beyond the position of the hump along the core distance, wherever applicable) with higher values of coefficient and slope of the exponential function (2). Moreover, the parameter β is smaller for iron primaries than for protons, i.e. for primary particle of higher mass composition the curvature is less.

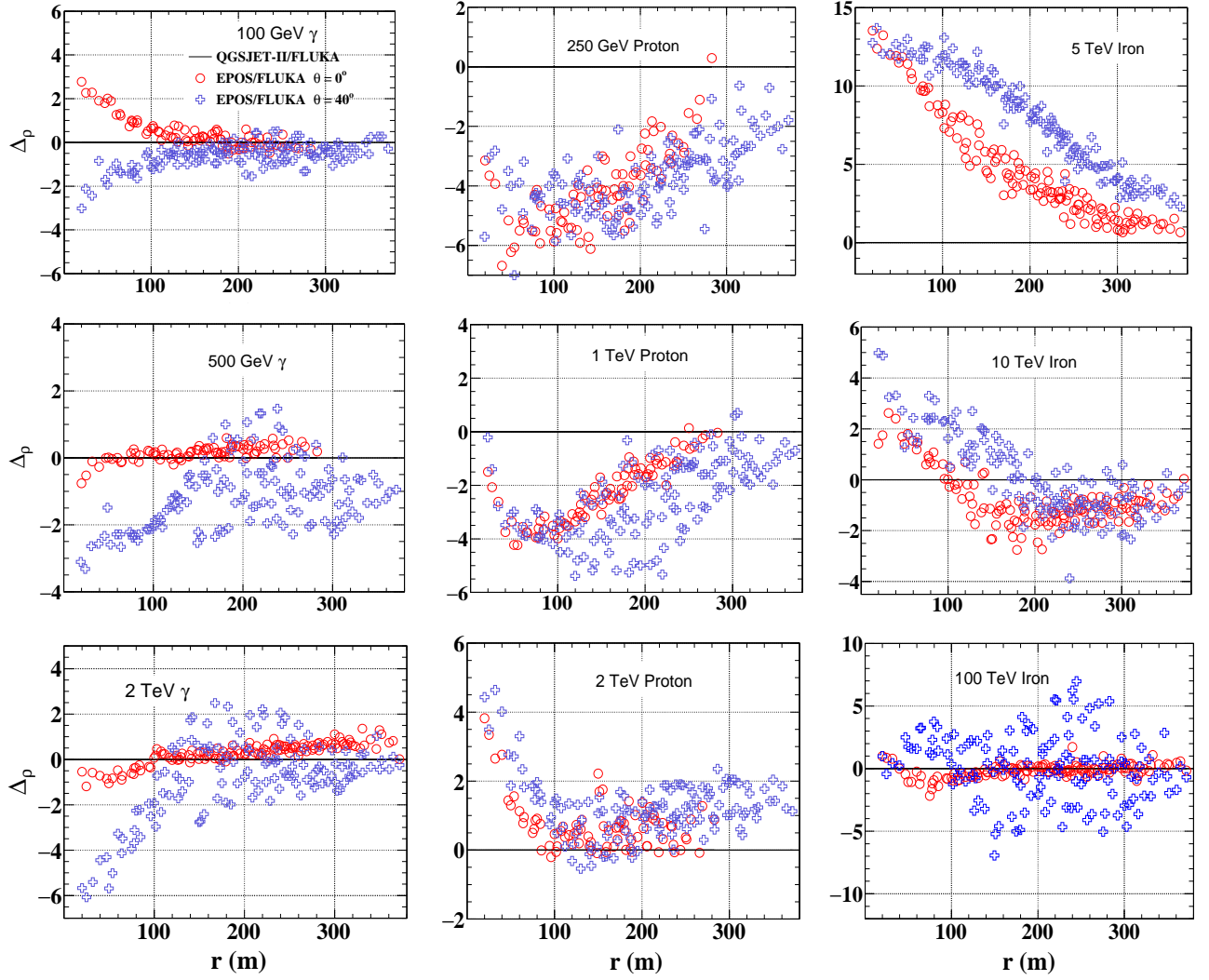


FIG. 2: % Relative deviation of Cherenkov photon densities ($\Delta\rho_s$) with respect to distance from the shower core of different primaries for the two high energy hadronic interaction models. The horizontal solid line in all plots indicates the QGSJETII-FLUKA model combination, which is considered as the reference for the calculation.

2. Hadronic interaction model sensitivity

To see the effect of the hadronic interaction models (used in this study) on the lateral density of the Cherenkov photons, we have calculated the % relative deviation of ρ_{ch} ($\Delta\rho$) for the EPOS-FLUKA model combination taking QGSJETII-FLUKA as the reference. Results are shown in the Fig.2 for the vertically incident and 40° inclined showers of different primaries with different energies only as representation. It is to be mentioned that, the choice of reference model combination is arbitrary and any one of the two may be used as the reference. For the γ -ray primaries, incident vertically at different energies, there is no significant differences in densities due to hadronic interaction models. Near to the shower core (< 100 m) some deviations of

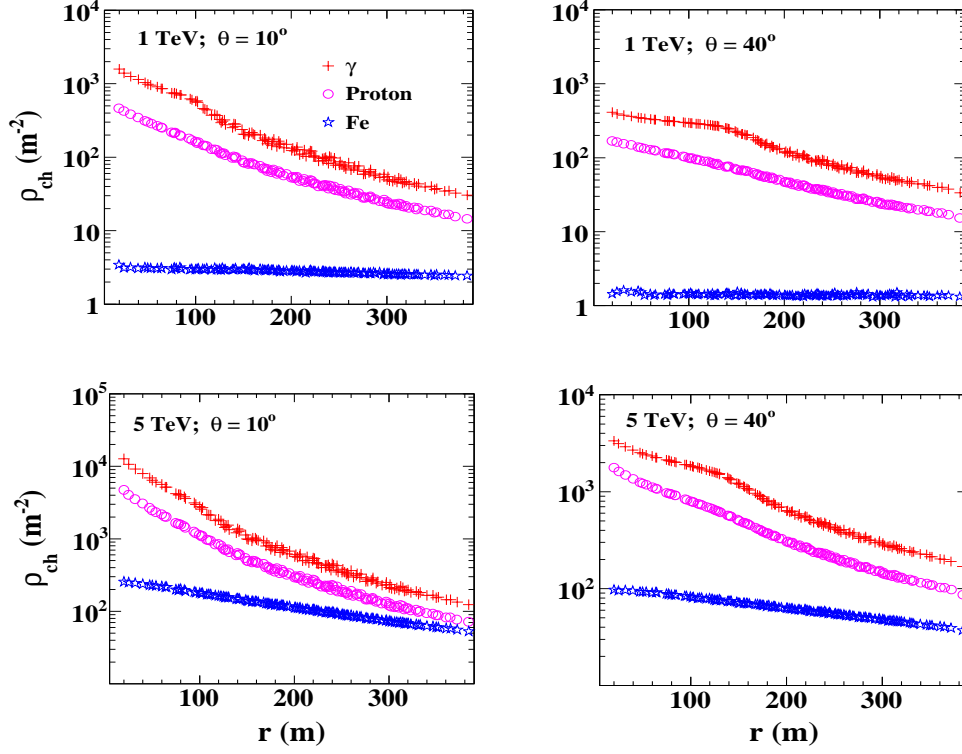


FIG. 3: Distributions of ρ_{ch} s with respect to distance from the shower core of γ , proton and iron primaries at 1 TeV and 5 TeV energies incident at 10° and 40° .

$\sim \pm 3\%$ are observed and beyond this distance the density deviations are within $\sim \pm 1\%$. However, for the inclined shower the density deviation is slightly higher (upto $\sim 6\%$), specially at higher energies.

For the case of proton primary, the deviation between the two models is clearly visible for both vertically incident and inclined showers, and is more significant in comparison to γ -ray primary. At lower primary energies these deviations are mostly negative and limited within $\sim 6\%$, while for higher primary energies they are mostly positive. In the case of 2 TeV primary, the deviations are mostly limited to $\sim 2\%$. For the 5 TeV primary with vertical incidence, the deviation extends from $\sim -3\%$ to $\sim 10\%$ and for the inclined shower it ranges from $\sim 2\%$ to $\sim 10\%$. Basically, only near the shower core (< 100 m), the deviation is high for both 2 TeV and 5 TeV primaries.

The deviation in density for the iron primaries are different from the γ and proton primaries, where the deviation is higher at lower primary energy. At 5 TeV energy, for both vertical and inclined showers, the deviation is maximum ($\sim 13\%$) near the shower core and gradually decreases with distance from the core to match with each other at the farthest points. For 10 TeV primary the deviation is mostly limited within $\sim \pm 2\%$ with the deviation becoming positive from negative near the core. With increasing energy, the deviation for the vertical shower decreases substantially in comparison to inclined shower. For example, at 100 TeV the two model exactly matches each other for the vertical shower while for the inclined shower, the deviation is distributed between $\sim \pm 6\%$. It is clear that, for all primary particles and energies, density deviation due to models is higher for the inclined shower than the vertical shower. However, as a whole on average, the range of deviation is within the acceptable limit ($< \pm 10\%$).

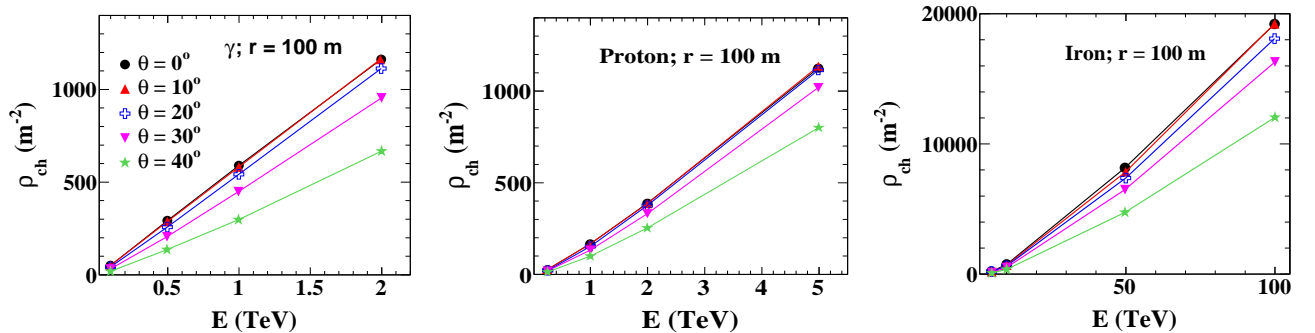


FIG. 4: ρ_{ch} s with respect to energy of the primary at a distance of 100 m from the shower core of γ , proton and iron primaries.

3. Nature of the fluctuation parameter (σ_{pm})

It is seen from the Fig.1 that for γ -ray primaries, the value of σ_{pm} of ρ_{ch} initially decreases with increase in core distance upto a distance of ~ 100 m and then gradually increases. This pattern continues for all energies and for vertical as well as inclined showers. Moreover, the value of σ_{pm} is found to become smaller with increase in energy of the primaries. Similar pattern in the variation of σ_{pm} is also observed for proton primaries. In case of proton, the values are much higher than γ -ray primaries with a decreasing trend with increase in energy of the primary. For iron primaries also, σ_{pm} decrease with increasing energy, however its value is much smaller than that of proton and, unlike proton and γ -ray primaries it remains almost constant for iron primaries with increasing core distance [1]. Furthermore, σ_{pm} is highest for the most inclined shower and least for the vertical shower in cases of all primaries, energies and almost for all core distances. This is due to the reason that, as inclination increases the shower has to travel gradually longer distance to reach the observation level, which creates increasing statistical fluctuation with increasing absorption of shower particles within the atmosphere.

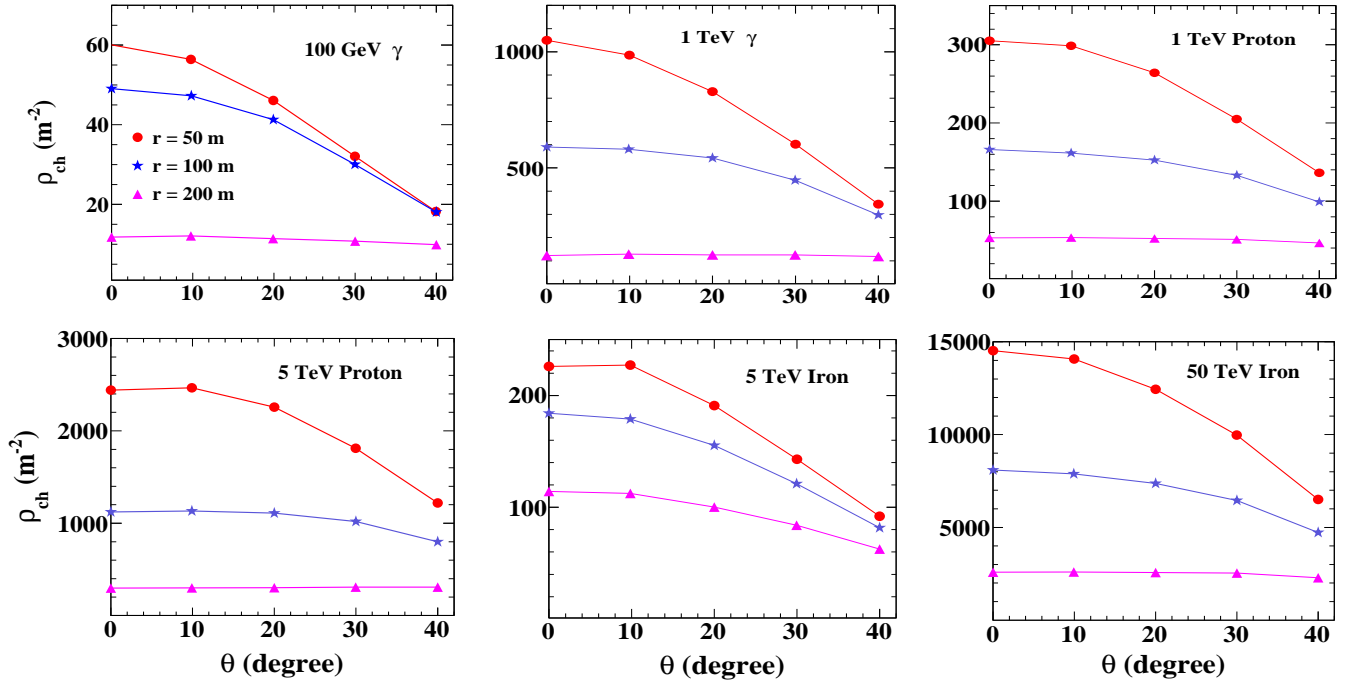


FIG. 5: ρ_{ch} s with respect to angle of incidence at 50 m, 100 m and 200 m from the shower core of γ , proton and iron primaries.

4. Variation of density with the primary particle and energy

It is quite obvious that, the γ -ray primary produces maximum number of Cherenkov photons and the iron primary produces the lowest number at a given energy and angle of incidence. This is mainly due to the fact that, almost all the energy of the γ -ray primary are utilized in the formation of electromagnetic shower, whereas for proton and iron primaries a portion of the energy is used up in the formation of hadronic shower along with the electromagnetic one. In Fig.3, the ρ_{ch} distributions with respect to the core distance produced by γ , proton and iron primaries of 1 TeV and 5 TeV inclined at 10° and 40° are shown to justify this result.

In the Fig.4 we have shown the variation of ρ_{ch} at core distance of 100 m with respect to energy for the all primary particles. It has been found that, for the γ -ray primary, the ρ_{ch} increases rapidly and linearly with the primary energy. Whereas in the cases of proton and specially of iron primaries, the increase is comparatively slow and non-linear with the primary energy. Moreover, this figure also indicates the result mentioned above.

5. Variation of density with angle of incidence

In Fig.5 the variation of density ρ_{ch} as a function of angle of incidence at distances from the core equal to 50 m, 100 m and 200 m is shown for all the three primaries at two different energies. It is quite clear that upto the distance of 50 m there is very small or no difference in density between vertically incident shower and shower inclined at 10° . However, beyond the angle of incidence 10° , the density falls off almost linearly for all combinations of primary particle and energy. At 200 m, the variation of density with angle of incidence is negligible, because only high energetic photons could reach at larger distances from the core over the observation level. At 100 m, the pattern of variation of photon density is in between the patterns of variation at 50

m and 200 m. The difference in densities at 50 m and 100 m decreases with increasing angle of incidence, but increases with primary energy. This difference is lowest for γ -ray primaries (in fact zero for 100 GeV γ at 40° angle of incidence) and highest for proton primary.

B. Arrival time of Cherenkov photons

1. General characteristics

The variation of mean arrival time of Cherenkov photons (t_{ch}) with respect to core distance has been studied from two perspectives: one with fixed angle of incidence and variable energy, while the other with fixed energy and five different angle of incidence. Some of the results are shown in the Fig.6 and Fig.7 respectively. It is seen that, the shower front is nearly spherical in shape for all primary particles, energies and angle of incidences. However, near the shower core (up to the core distance of ≤ 100 m), t_{ch} with respect to core distance increases slowly and after that the rate of its increase is comparatively rapid. As a result, the shape of the distribution deviates slightly from the spherical symmetry. It is clear from the Fig.6 that, for all values of angle of incidence, the value of t_{ch} increases with increase in energy of the primary. From the figure Fig.7 it can be seen that, as the angle of incidence increases, the value of t_{ch} decreases for all combinations of energy and primary. Moreover, it is also evident from these figures that for vertically incident as well for inclined showers the arrival time follows very similar pattern. It is found that for all combinations of energy and angle of incidence irrespective of the primary particle, the variation of t_{ch} can be represented by an equation of the form [1]:

$$t_{ch}(r) = t_0 e^{\Gamma/r^\lambda}, \quad (3)$$

where $t_{ch}(r)$ is the position dependent arrival time, r is the distance from the shower core, t_0 , Γ and λ are constant parameters of the function. The values of these constant parameters depend on the type and energy of the primary particle for a given angle of incidence. In the Fig.6 the best fit functions are shown as solid lines for one of the energy corresponding to the different angle of incidence. The method used for the fitting is same as that used for the density distributions.

2. Hadronic interaction model sensitivity

As in the case Cherenkov photon density mentioned above, for a better idea about the effect of the hadronic interaction models on the arrival time of Cherenkov photons with respect to shower core for various combinations of primary particle, energy and angle of incidence, we have studied the relative deviations in the t_{ch} s considering QGSJETII-FLUKA combination as the reference model. Fig.8 shows the % relative deviations of the arrival time (Δ_t) of the shower front obtained from the EPOS-FLUKA model combination for various mono energetic primary particles, incident vertically and at an angle 40° . From the figure it is clear that, the differences in the t_{ch} s due to two model combinations are very small (0 to $\sim \pm 6\%$) for all the vertically incident primaries, except for the high energy iron primaries, where deviation goes beyond $\pm 10\%$. Whereas for the inclined showers there is almost no difference between the two models except for iron primaries at higher energies. For example, at 100 TeV iron primary with 40° angle of incidence the deviation lies in between $\sim -4\%$ to -10% . Moreover, for the vertical showers, the difference between the two models is remarkable mainly for the core distances below 100 m, beyond which the % relative variation in arrival time is quite small, mostly less than $\pm 2\%$. Although no specific trend has been observed in the deviation pattern of the arrival time due to the two models for vertical showers, however it is quite interesting to see that the two models behaves exactly the same for the showers inclined at 40° .

3. Nature of the fluctuation parameter (σ_{pm})

We have calculated σ_{pm} of arrival time for all three primaries having different energy and angle of incidence combination, like we did for the density fluctuation and these are plotted in the Fig.6 to see the fluctuations in the t_{ch} distributions. It is clearly visible that, for the vertically incident showers irrespective of the primary particle and the energy combination, the fluctuation is large near the core for distances below 100 m and then σ_{pm} has a decreasing pattern with increase in distance from the core. The proton primary shows maximum fluctuation (highest at 250 GeV) and the iron shows the least. However, for the rest of the cases i.e. for all the inclined showers, the σ_{pm} is smaller near the core and gradually increases with increase in distance from the shower core. It appears from the figure that for the inclined showers, the fluctuation is almost independent of primary particle, its energy and the angle of incidence.

4. Variation of arrival time with the primary

In Fig.9, the arrival time as a function of distance from the core is plotted for the three primaries of same energy (in each plot) inclined at 10° and 40° . It is seen that Cherenkov photons initiated by γ -ray primaries take more time than that of proton and iron primaries to reach the detection level. Though γ -ray primaries and proton primaries show very similar pattern, but the

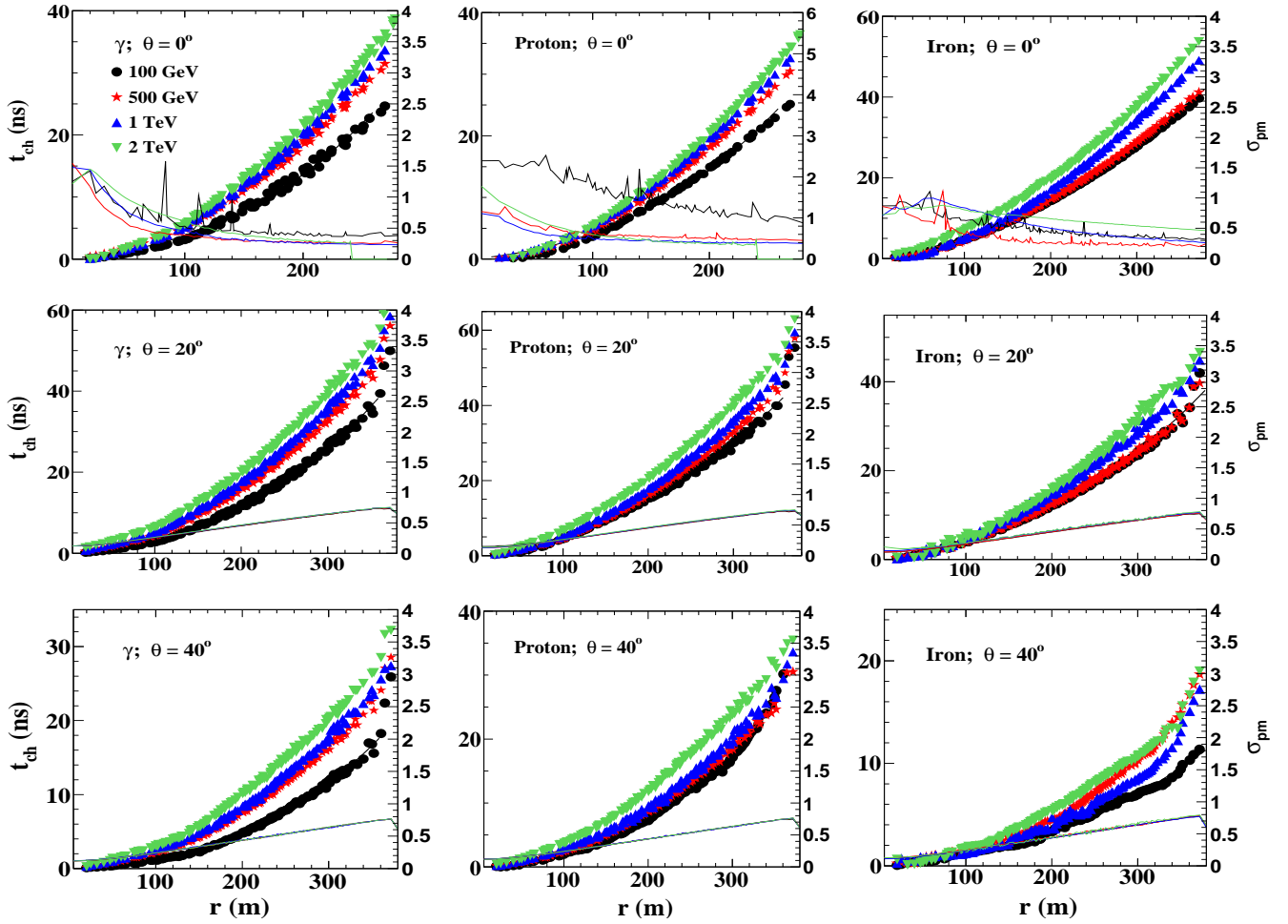


FIG. 6: Variations of average arrival times of Cherenkov photons (t_{ch}) and their σ_{pm} with respect to distance from the shower core of different primaries at different energies corresponding to some fixed value of angle of inclination. The solids line indicate the results of the best fitted function (3) to the respective plots for any one of the energy.

iron primary initiated photons distinctly take lower time to reach the detectors. The trend continues for all the energy and angle of inclination combinations. This is not surprising result because, we have already seen that, the number Cherenkov photon produce by γ -ray primary at a particular energy is very large in comparison to iron primary and slightly large in comparison to the proton primary. So, at a given energy, the γ -ray initiated shower takes distinctly long average time than the iron initiated shower and slightly longer average time than the proton primary to reach the observation level.

5. Variation of arrival time with the angle of incidence

The variations of arrival times with the angle of incidence for γ -ray, proton and iron primaries are shown in Fig.10. This figure shows only the plots for two different energies of each primary at a core distance of 50 m, 100 m and 200 m. It is observed that, there is a overall falling trend of arrival time with respect to angle of incidence for all primary particles, energies and at all core distances. At low energy, this trend is almost steady for all primary particles. But at high energy, it is not so steady or smooth. In case of γ -ray primaries the trend is most smooth, whereas it is least smooth in the case of iron primaries. This is due to the reason that the air shower produce by a γ -ray primary is homogeneous in nature, on the other hand air shower produce by a iron primary is most inhomogenous. Moreover, with the increasing distance from the shower core, the rate of falling of the t_{ch} increases with the angle of incidence. Since at large angle of incidence, only few very high energetic particles can reach over a large distance from the shower core, so the average arrival time decreases rapidly with the incidence angle in a such case.

6. Variation of arrival time with the energy of the primary

In the Fig.11 we have shown the variation of t_{ch} at a distance of 100 m from the core with energy of the γ -ray, proton and iron primaries incident at different zenith angles. In the cases of γ -ray and proton initiated showers, t_{ch} is found to increase with increase in energy for almost all angle of incidence. However, for the proton primary incident at angle of 20° there is a slight exception below the energy of 1 TeV. Moreover, for vertically incident shower of both these primaries, rate of increase of t_{ch}

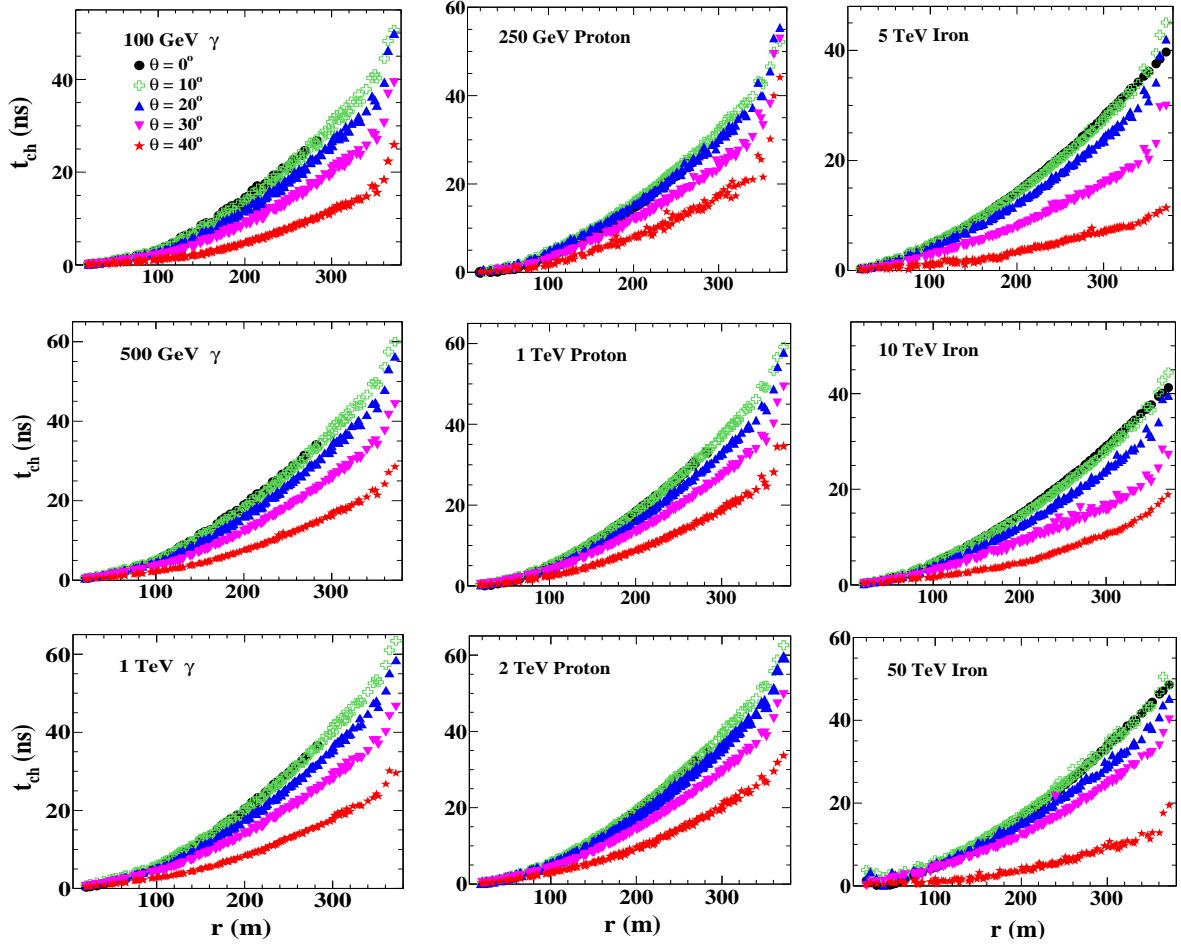


FIG. 7: Variations of average arrival times of Cherenkov photons (t_{ch}) with respect to distance from the shower core of different primaries at different angle of inclination corresponding to some fixed value of energy.

becomes very small after certain value of the energy of each primary. Very slight similar trend is also shown by the showers of both these primary incident at 10° . For iron primaries, there is a decrease in t_{ch} first, then there is a very slow increase in it with the increase in energy, but an exception is seen for the vertically incident primary, where there is a reduction in the t_{ch} with increase in energy. Almost similar situation is also observed for the iron primary incident at 10° with energy above 50 TeV. Notwithstanding, overall, at a distance of 100 m from the shower core there is a increasing tendency in the average arrival time with increase in energy of the primary with few exceptions.

C. Angular distribution of Cherenkov photons

1. General characteristics

The angular distribution of Cherenkov photons is obtained by counting the number of photons produced per angular bin ($\frac{dN}{d\theta}$ (degree $^{-1}$)) with respect to the shower axis. Some of the angular distributions are shown in the Fig.12 for various combinations of energy and angle of incidence for all the three primaries. These distributions are found to follow certain peculiar trends for almost all the combinations. It is seen that, for any value of angle of incidence the distribution becomes increasingly flatter and wider with increase in energy of the primary. This behaviour clearly suggests that as energy of the primary increases, the number of particles deflected at larger angles from the shower core also increases. Moreover, this tendency of the distribution is most prominent for the γ -ray shower and least prominent in the case of iron shower. This is because, the electromagnetic component of the shower, which is deflated most and is responsible for the production of Cherenkov photons, produced by the iron primary is the lowest, whereas the shower produced by γ -ray primary is wholly electromagnetic. It has been also observed that for a particular energy of the primary, the angular profile becomes increasingly narrower as the angle of incidence of primary increases. Also, from the 20° angle of incidence, the distribution profile becomes symmetric about the angle of incidence and with the increasing angle of incidence, effect of energy of the primary particle becomes gradually insignificant, specially for the proton and iron primaries. Furthermore, it is seen that the Cherenkov photon density falls off almost linearly with the increasing angle about the shower axis.

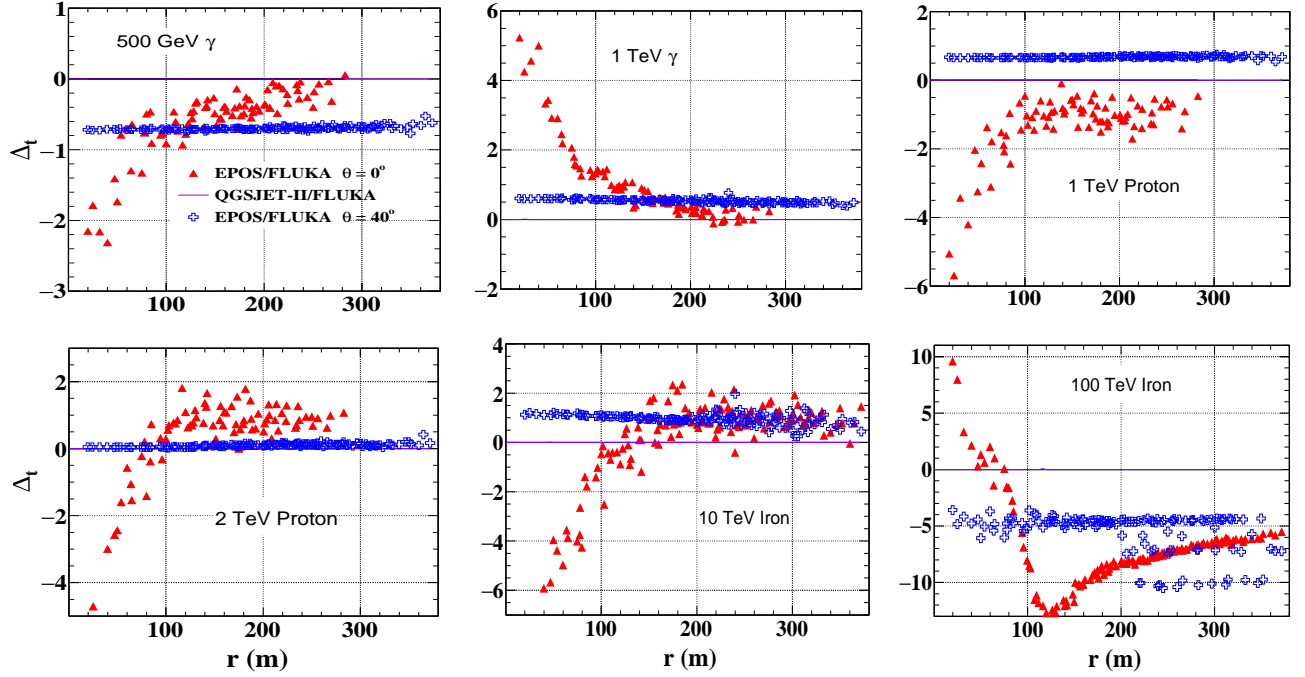


FIG. 8: % Relative deviation of Cherenkov photon arrival times (Δt_{ch} s) with respect to distance from the shower core of different primaries for the two high energy hadronic interaction models. The horizontal solid lines in all plots indicate the QGSJETII-FLUKA model combination, which is considered as the reference for the calculation.

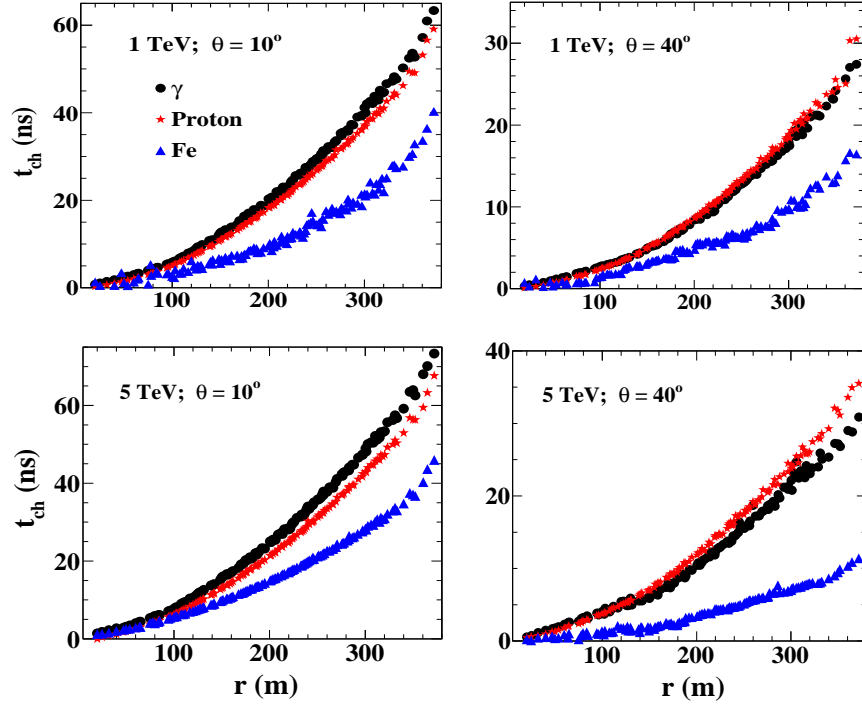


FIG. 9: Variation of t_{ch} with respect to distance from the shower core for γ , proton and iron primaries of equivalent energy.

2. Hadronic interaction model sensitivity

The angular distributions of Cherenkov photons as obtained from the EPOS-FLUKA and QGSJET-FLUKA model combinations are shown the Fig.13. It is observed that, there is hardly any difference between the results obtained from the two models. However, for the iron primaries of energy 100 TeV incident at angles 20° , 30° and 40° there are some differences between the two models.

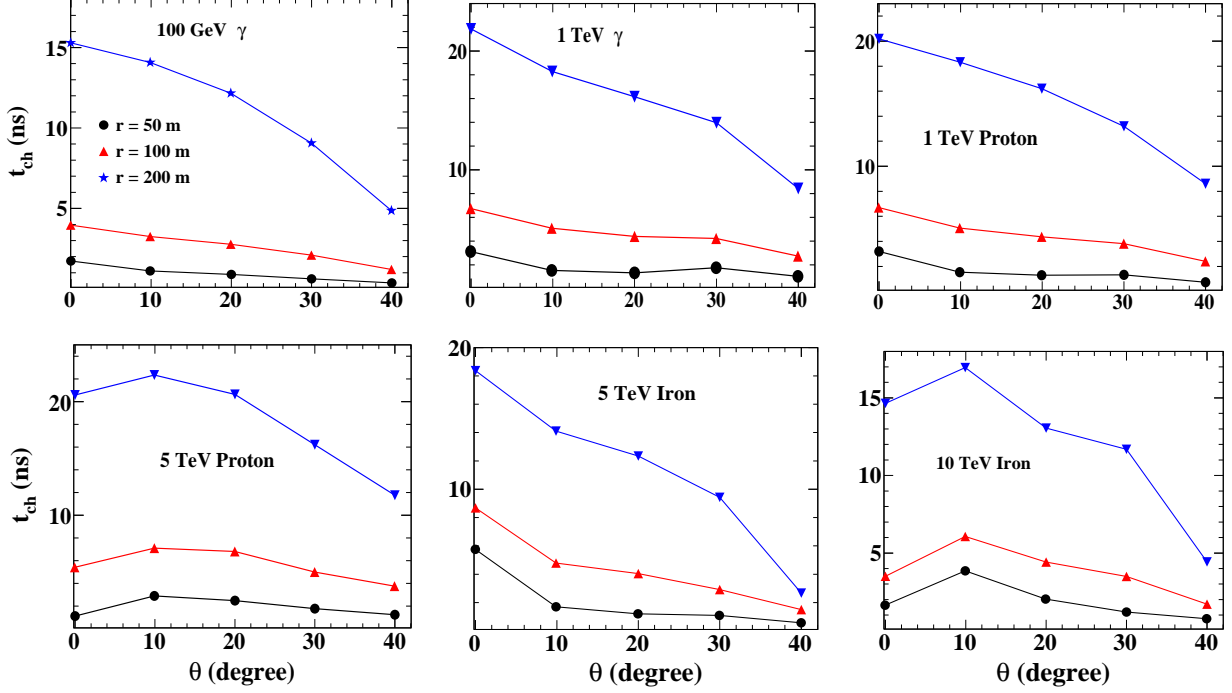


FIG. 10: Variations of t_{ch} s with respect to angle of incidence at 50 m, 100 m and 200 m from the shower core of γ , proton and iron primaries.

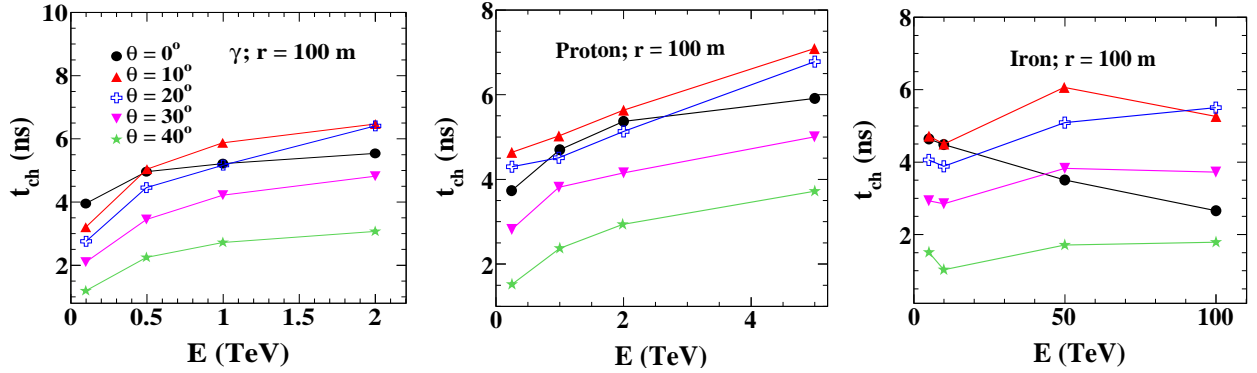


FIG. 11: Variations of t_{ch} with respect to energy of the primary at a distance of 100 m from the shower core for γ , proton and iron primaries.

3. Variation of angular distribution with the primary

To see clearly the effect of the primary particle on the angular distribution pattern, we have plotted the angular distributions of the Cherenkov photons in the showers of γ -ray, proton and iron primaries for two different energies incident at two different zenith angles in the Fig.14. As already mentioned above, it is seen that Cherenkov photons initiated by γ -rays are distributed in wider angular range than in comparison to proton and iron primaries irrespective of energy and angle of incidence. Cherenkov photons initiated by iron primaries are confined within the smallest angular range.

IV. SUMMARY AND CONCLUSION

Considering the importance of effective gamma hadron separation techniques in ACT and the lack of sufficient studies in the corresponding area, we have studied the density, arrival time and angular distributions of Cherenkov photons in EASs of vertically incident as well as inclined γ -ray, proton and iron primaries at different energies using the CORSIKA 6.990 simulation package [8]. This is the sequel of our earlier work [1] to generalize the study in extending energy and zenith angles of primary particles.

The density of Cherenkov photons increases with energy for all primaries and decreases exponentially with increase in distance from the shower core. This is an obvious experimental fact that at a particular observation level it is easy to detect a high energy shower than a low energy shower and for a proper estimation of energy of a shower, the shower has to incident well within the detector array. Also with increase in angle of inclination, the density decreases almost linearly. This result also supports

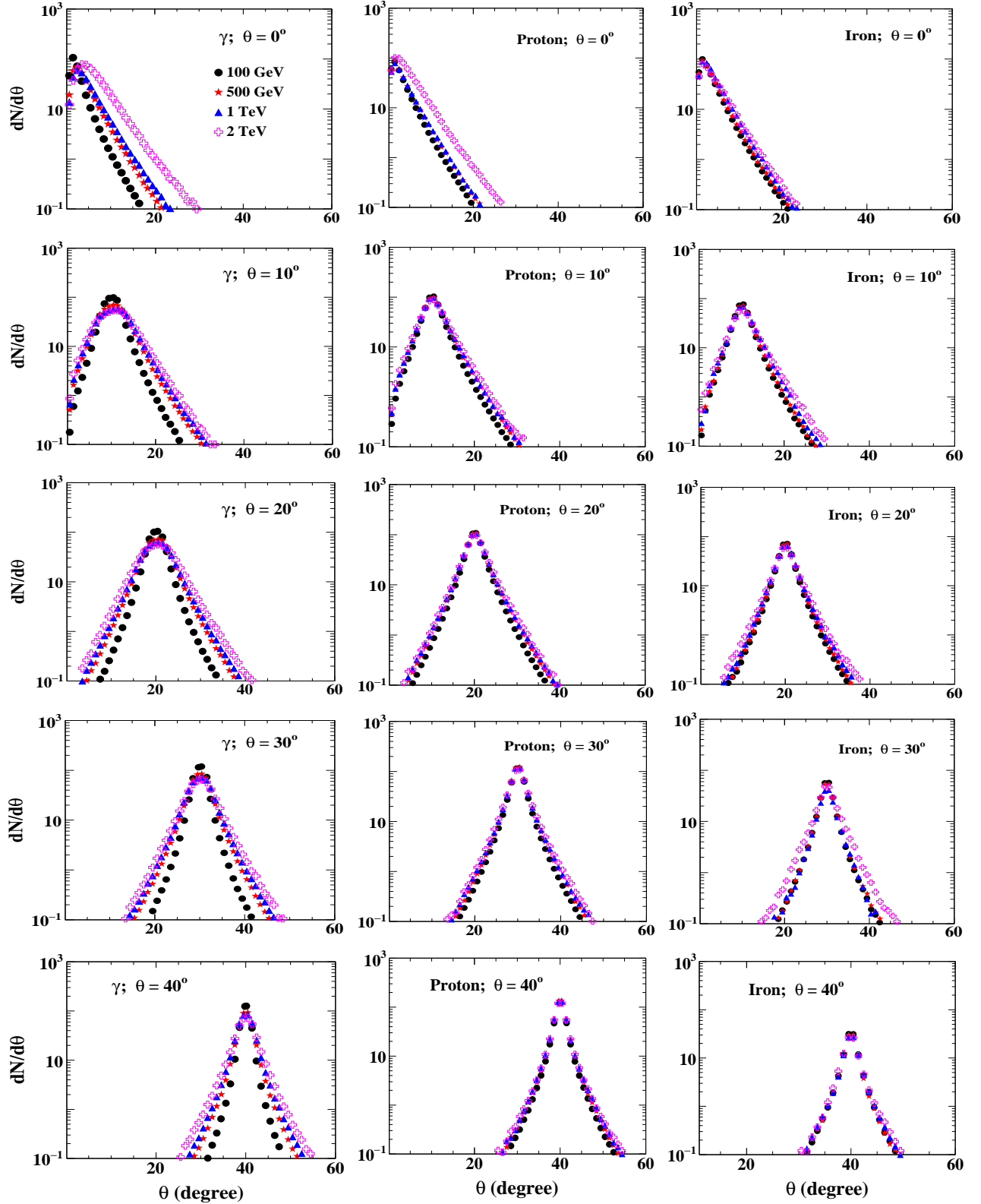


FIG. 12: Angular distributions of Cherenkov photons obtained from different primaries at different energies corresponding to some fixed value of angle of inclination of primary particle.

well known observational situation that, it is hard to detect an inclined than a vertical shower of same energy. γ -rays have the highest Cherenkov photon yield followed by proton and iron for any combination of energy, angle and hadronic model. Thus, the equivalent energy of the iron primary must be highest followed by proton and γ -ray for a given Cherenkov photon yield for any cited combination.

The average arrival time of Cherenkov photon is found to increase according to an exponential function (see equation (3)) with increase in distance from the shower core for all combinations of energy and angle of incidence. With increase in energy, the general trend shows an overall increase in the arrival time for all primaries, except for the vertically and the near vertically

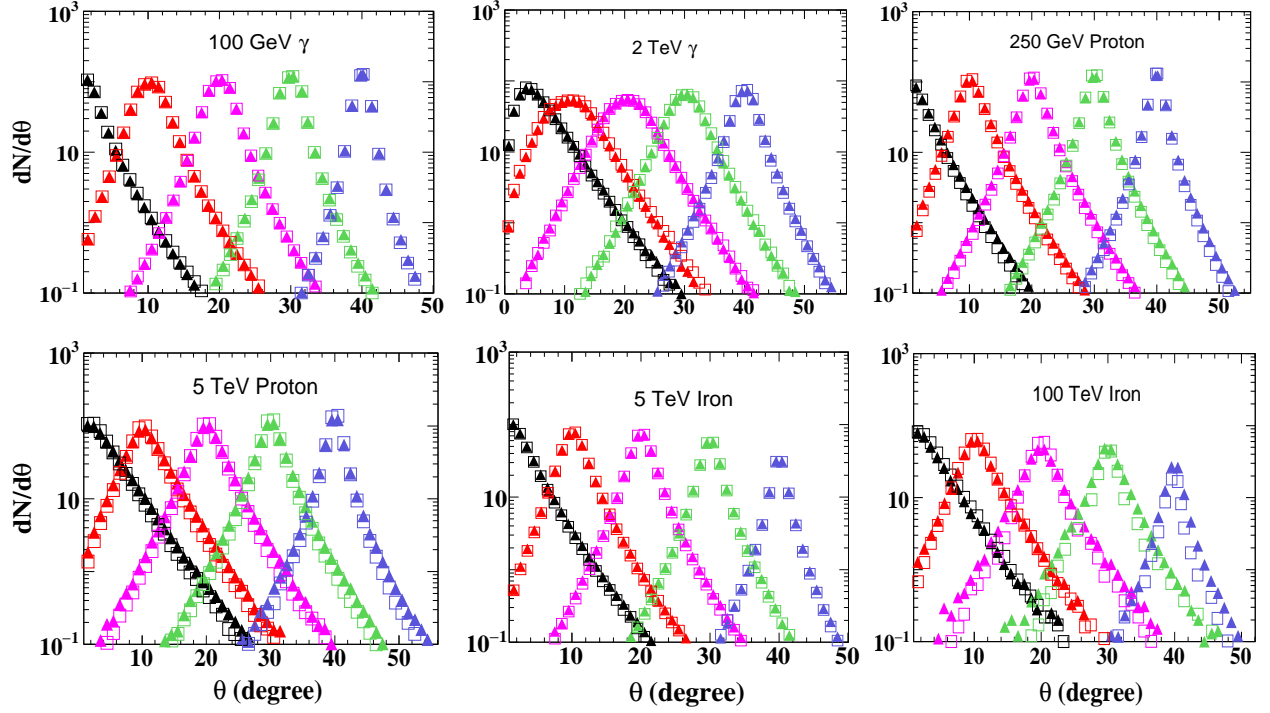


FIG. 13: Angular distributions of Cherenkov photons from different primaries as obtained by EPOS-FLUKA and QGSJETII-FLUKA model combinations. In the plots, different coloured \bullet and \square indicate the EPOS-FLUKA and QGSJETII-FLUKA model combinations respectively. Plots with peaks from left to right represent the showers with zenith angles from 0° to 40° respectively.

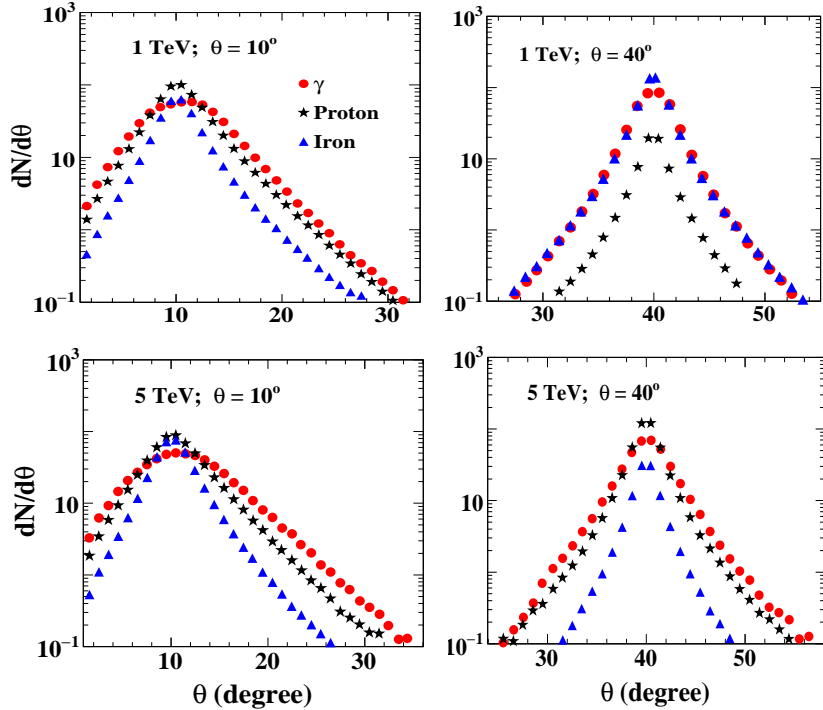


FIG. 14: Angular distributions of Cherenkov photons obtained from different primaries with two different energies and angles of incidence.

incident iron primary, in which case the trend is opposite. However, with the increase in angle of incidence the arrival time profile becomes flatter and hence there is a decrease in arrival time. At a particular energy and an angle of incidence, the arrival time is highest for the γ -ray primary and least for the iron primary. All these information along with the features of density distribution may be useful to disentangle the γ -ray showers from the hadronic showers while analyzing the experimental EAS data, apart from usual determination of direction of a shower from the arrival time information.

In general, the shower to shower fluctuation in density and arrival time of Cherenkov photons decreases with increasing energy of primary particle, and is highest for proton primary and least for the γ -ray primary at all angle of incidence. While estimating

the systematic uncertainties in the data of γ -ray experiment, these information will provide an important input to be taken care.

In the case of angular distributions, most of the photons are arriving within 1° or 2° about its shower axis, beyond which the density per angular bin falls off rapidly depending upon the energy, type and angle of incidence of the primary particle. The angular distribution patterns show distinct variation between γ -ray, proton and iron primaries so as in the density and arrival time profile. The proper parametrization of this distinction in the distribution patterns will be useful for distinguishing the γ -rays from the CR background.

Moreover, the QGSJETII-FLUKA and EPOS-FLUKA model combination produces almost similar results in the density, arrival time and angular distributions. So, any of these two high energy models can be use to analyze the experimental data of γ -ray astronomy.

We feel that, a full scale parametrization of the density, arrival time and angular distribution of Cherenkov photons for different primary at different angle of incidence will be helpful for complete understanding of the interdependence of the various sensitive parameters, which may eventually lead to the most effective gamma-hadron separation techniques. We hope to report such work in future as a part of complete simulation study on atmospheric Cherenkov photons.

-
- [1] P. Hazarika, U. D. Goswami, V. R. Chitnis, B. S. Acharya, G. S. Das, B. B. Singh, R. Britto, *Astroparticle Physics* **68**, 16 (2015) [arXiv:1404.2068].
 - [2] René A. Ong, *Phys. Reports* **305**, 93 (1998); C. M. Hoffman and C. Sinnis, *Rev. Mod. Phys.* **71**, 897 (1999); T. C. Weekes, *astroph/0811.1197v1* (2009); P. N. Bhat, *Bull. Astr. Soc. India* **30**, 135 (2002); B. S. Acharya, 29th ICRC, **10**, 271 (2005).
 - [3] H. M. Bardan, T. C. Weekes, *Astropart. Phys.* **7**, 307 (1997); Herve Cabot et al., *Astropart. Phys.* **9**, 269 (1998).
 - [4] V. R. Chitnis, P. N. Bhatt, *Astropart. Phys.* **15**, 29 (2001).
 - [5] A. M. Hillas, *J. Phys. G: Nucl. Phys.* **8**, 1461 (1982).
 - [6] S. Lafebre, R. Engel, H. Flacke, J. Horandel, T. Huege, J. Kuijpers, R. Ulrich, *Astropart. Phys.* **31**, 243 (2009).
 - [7] F. Nerling, J. Blumer, R. Engel, M. Risse, *Astropart. Phys.* **24**, 421 (2006).
 - [8] J. Knapp, D. Heck, *EAS Simulation with CORSIKA V 6990: A User's Guide* (1998); D. Heck et al., Report **FZKA 6019** (1998), Forschungszentrum Karlsruhe; http://www.wik.fzk.de/corsika/physicsdescription/corsika_phys.html
 - [9] W. R. Nelson, H. Hirayamal, D. W. O. Rogers, *The EGS4 Code System*, SLAC Report 265 (1985).
 - [10] T. Pierog, K. Werner, *Nucl. Phys. Proc. Suppl.* **196**, 102 (2009) [arXiv:0905.1198].
 - [11] US Standard Atmosphere (US Govt. Printing Office, Washington, 1962).
 - [12] <http://root.cern.ch>